VNU Journal of Science: Natural Sciences and Technology, Vol. 31, No. 4 (2015) 68-76

Zeta Potential Measurement Using Electroosmosis in Porous Media

Lương Duy Thành[1,*], Rudolf Sprik[2]

[1]*Water Resources University, 175 Tây Sơn, Đống Đa, Hanoi, Vietnam*

[2]*Van der Waals-Zeeman Institute, University of Amsterdam, 1098XH Amsterdam, The Netherlands*

Received 13 April 2015
Revised 4 May 2015; Accepted 22 August 2015

Abstract: The zeta potential of a solid-liquid interface in porous media is an important surface characterization quantity for geophysical applications or environmental applications, for example. The zeta potential in porous media is normally measured by some techniques such as streaming potential, streaming current. In this work, we use electroosmosis to measure the zeta potential for consolidated porous samples including natural and artificial rocks saturated with NaCl solutions. The measurements show that the values of the zeta potential deduced from our electroosmosis measurements are always smaller than those of the corresponding samples deduced from the reliable streaming potential measurements in literature, in particular for the low permeability samples. The reason may be that the samples are not fully saturated by liquid (in particular for low permeability samples) or the degradation of electrodes happens. The result suggests that the electroosmosis measurements are not a promising method to determine the zeta potential in porous media.

Keywords: Electroosmosis, streaming potential, zeta potential, porous media.

1. Introduction

Electrokinetic phenomena in a porous medium are the result of a coupling between fluid flow and electric current flow. Electrokinetic phenomena consist of several different effects such as streaming potential, electroosmosis etc. (e.g., see [1]).

Streaming potential that arises due to fluid moving through porous media plays an important role in geophysical applications. For example, streaming potential could be used to map subsurface flow and detect subsurface flow patterns in oil reservoirs (e.g., [2-8]), geothermal areas and volcanoes (e.g., [9-14]). Monitoring of streaming potential anomalies has been proposed as a means of predicting earthquakes (e.g., [15-17]).

Electroosmosis that arises due to the motion of liquid induced by an applied voltage across a porous material is one of the promising technologies for cleaning up low permeable soil in environmental applications. In this process, contaminants are separated by the application of an electric field between two electrodes inserted in the contaminated mass. Therefore, it has been used for the removal of organic

* Corresponding author. Tel.: 84-936946975.
Email: luongduythanh2003@yahoo.com

contaminants, petroleum hydrocarbons, heavy metals and polar organic contaminants in soils, sludge and sediments (e.g., [18-20]). The zeta potential of a solid-liquid interface of porous media is one of the most important parameters in electrokinetic phenomena. It is normally deduced from streaming potential, streaming current measurements. In this work, we use electroosmosis to calculate the zeta potential for consolidated porous samples including natural and artificial rocks saturated with NaCl solutions. The measurements show that the values of the zeta potential deduced from our electroosmosis measurements are always smaller than those of the corresponding samples deduced from the reliable streaming potential measurements in literature, in particular for the low permeability samples. The reason may be that the samples are not fully saturated by liquid (in particular for low permeability samples) or the degradation of electrodes happens. The result suggests that the electroosmosis measurements are not a promising method to determine the zeta potential in porous media.

This work includes five sections. Section 2 describes the theoretical background of electrokinetics. Section 3 presents the experimental setup for electroosmosis measurement. Section 4 contains the experimental results and discussion. Conclusions are provided in Section 5.

2. Theoretical background of electrokinetics

2.1. Electric double layer

Electrokinetic phenomena are induced by the relative motion between the fluid and a charged surface under application of an external force, and they are directly related to the existence of an electric double layer (EDL) between the fluid and the solid surface [1, 21, 22]. This external force might be electric, pressure gradient, concentration gradient, or gravity. A porous medium is formed by mineral solid grains such as silicates, oxides, and carbonates (Fig. 1).

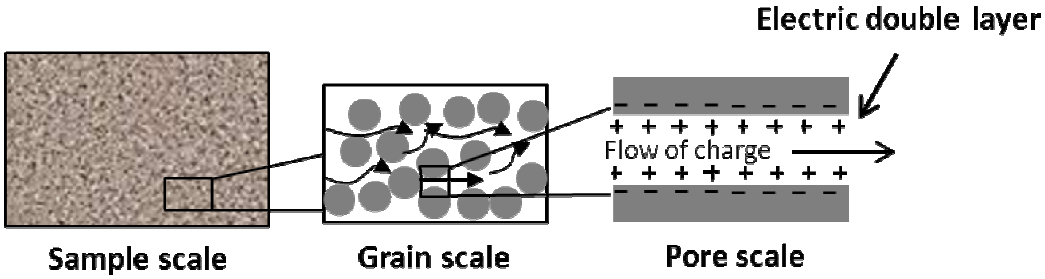

Figure 1. Schematic of the porous medium with different length scales: sample scale, grain scale and pore scale.

When a solid grain surface is in contact with a liquid, it acquires a surface electric charge [22]. The surface charge repels ions in the electrolyte whose charges have the same sign as the surface charge (called the ”coions”) and attracts ions whose charges have the opposite sign (called the ”counterions” and normally cations) in the vicinity of the electrolyte-silica interface. This leads to the charge distribution known as the EDL (Fig. 2).

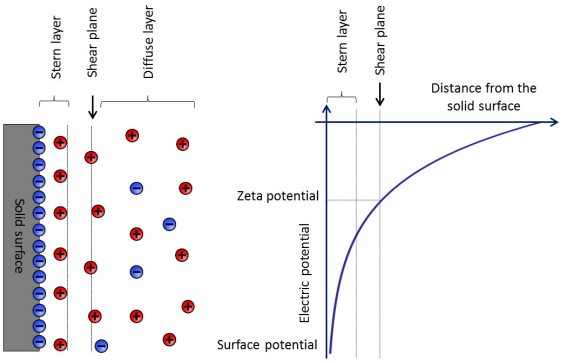

Figure 2. Stern model [27, 28] for the charge and electric potential distribution in the electric double layer at a solid-liquid interface.

In this figure, the solid surface is negatively charged and the mobile counter-ions in the diffuse layer are positively charged (in most rock-water systems) [23, 24].

The EDL is made up of the Stern layer, where cations are adsorbed on the surface and are immobile due to the strong electrostatic attraction, and the diffuse layer, where the ions are mobile. The distribution of ions and the electric potential within the diffuse layer is governed by the Poisson-Boltzmann (PB) equation which accounts for the balance between electrostatic and thermal diffusion forces [22]. The solution to the linear PB equation in one dimension perpendicular to a broad planar interface is well-known and produces an electric potential profile that decays approximately exponentially with distance as shown in Fig. 2. In the bulk liquid, the number of cations and anions is equal so that it is electrically neutral. The closest plane to the solid surface in the diffuse layer at which flow occurs is termed the shear plane or the slipping plane, and the electrical potential at this plane is called the zeta potential (ζ). The zeta potential plays an important role in determining magnitude of electrokinetic phenomena. Most reservoir rocks have a negative surface charge and a negative zeta potential when in contact with ground water [23, 24]. The characteristic length over which the EDL exponentially decays is known as the Debye length and is on the order of a few nanometers for typical grain electrolyte combinations [25, 26].

2.2. Electroosmosis

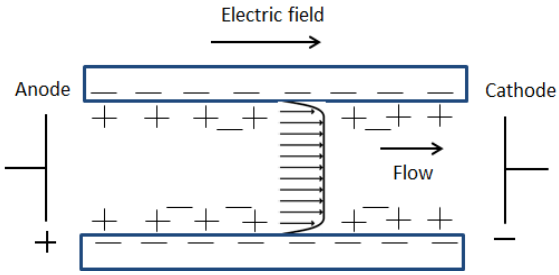

Figure 3. Electroosmosis flow in a capillary tube.

Electroosmosis was first observed by Reuss in 1809 in an experiment where a direct current was applied to a clay-sand-water mixture in a U-tube [29]. When an electric field is applied parallel to the wall of a capillary, ions in the diffuse layers experience a Coulomb force and move toward the electrode of opposite polarity, which creates a motion of the fluid near the wall and transfers momentum via viscous forces into the bulk liquid. So a net motion of bulk liquid along the wall is created and is called electroosmotic flow (see Fig. 3). The pressure necessary to counterbalance electroosmotic flow is termed the electroosmotic pressure [22].

A complex porous medium (see Fig. 1) with the physical length L and cross sectional area A can be approximated as an array of N parallel capillaries with inner radius equal to the mean pore radius a of the medium and an equal value of zeta potential ζ. For each of these idealized capillaries, the solution for electro-osmosis flow

in a single tube can be analyzed to estimate the behavior of the total flow in a porous medium by integrating over all pores [30].

In a U-tube experiment, when an electric potential difference is applied across the fluid saturated porous medium, the liquid rises on one side (the cathode compartment for our experiment) and lowers on the other side (the anode compartment). This height difference increases with the time and this process stops when the hydraulic pressure caused by the height difference equals the electroosmosis pressure (see Fig. 4). At that time the height difference is maximum.

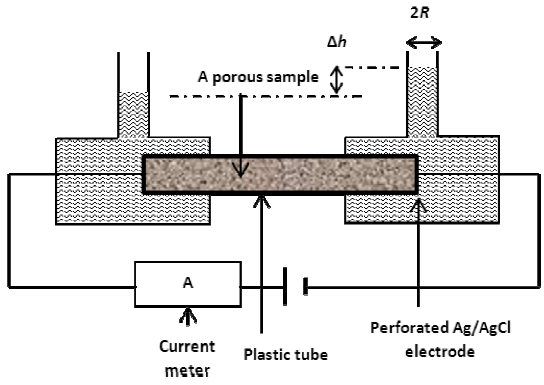

Figure 4. Schematic illustration of electroosmosis measurements in which Δh and R are height difference of liquid, the radius of the tubes in both sides, respectively.

The expression for the height difference as function of time is given by [18]

$$\Delta h = \frac{\Delta P_{eq}}{\rho_f g}\left[1-\exp(-\frac{N\rho_f g a^4}{4\mu R^2 L}t)\right] = \frac{\Delta P_{eq}}{\rho_f g}\left[1-\exp(-\frac{t}{\tau})\right], \quad (1)$$

$$\text{with } \Delta P_{eq} = \frac{8\varepsilon_r\varepsilon_o|\zeta|V}{a^2}\left[1-\frac{2\lambda I_1(a/\lambda)}{aI_o(a/\lambda)}\right], \quad (2)$$

$$\text{and } \tau = \frac{4\mu R^2 L}{N\rho_f g a^4}, \quad (3)$$

where τ is response time, ΔP_{eq} is the pressure difference caused by the electroosmosis flow at equilibrium which corresponds to maximum height difference, ρ_f is the fluid density, g is the acceleration due to gravity, V is the applied voltage across the porous medium, ε_r is the relative permittivity of the fluid, ε_0 is the dielectric permittivity in vacuum, λ is the Debye length, R is the radius of the tubes in both sides, I_0 and I_1 are the zero-order and the first order modified Bessel function of the first kind, respectively.

For a conductive liquid such as distilled water, the Debye length λ, is about few nm [18] and a typical pore radius of the samples used in this work (a), is around 4 μm. In this case the ratio $I_1(a/\lambda)/I_0(a/\lambda)$ can be neglected [31]. Under these conditions, Eq. (2) may be simplified as

$$\Delta P_{eq} = \frac{8\varepsilon_r\varepsilon_o|\zeta|V}{a^2}, \quad (4)$$

and Eq. (4) can be rewritten as follows

$$\Delta h = \frac{8\varepsilon_r\varepsilon_o|\zeta|V}{\rho_f g a^2}\left[1-\exp(-\frac{t}{\tau})\right] = \Delta h_{\max}\left[1-\exp(-\frac{t}{\tau})\right], \quad (5)$$

$$\text{with } \Delta h_{\max} = \frac{8\varepsilon_r\varepsilon_o|\zeta|V}{\rho_f g a^2} \quad (6)$$

3. Experiment

Electroosmosis measurements have been performed on 6 consolidated samples (see Table 1). The samples numbered from 1 to 3 are the natural ones obtained from Shell company in the Netherlands. The samples numbered from 4 to 6 are the artificial ones obtained from HP Technical Ceramics Company in England. The samples have a length of 55 mm and a diameter of 25 mm. The mineral composition of the

samples is reported by the manufacturers as shown in the Table 1.

Microstructure parameters of the porous samples such as permeability, porosity, formation factor, tortuosity and solid density have been measured in the work of Luong and Sprik [32] for streaming potential measurements and are rewritten in Table 1.

When using low electrical conductivity solutions such as deionized water, the effect is large. However, the electrical conductivity of the saturated samples slowly stabilizes in about 20 h for our samples. Perhaps due to CO_2 uptake from the air, that changes the conductivity. We therefore use a 10^{-3} M NaCl solution of low enough conductivity of 10×10^{-3} S/m measured by the conductivity meter (Consort C861) for the measurements. The pH of the solution, measured with the pH meter (Consort C861), is in the range 6.0 to 7.5. The measurements are carried out at room temperature (20°C).

Table 1. Sample ID, mineral composition and microstructure parameters of the samples. Symbols k_o (in mD), Φ (in %), F (no units), α_∞ (no units), ρ_s (in kg/m^3) stand for permeability, porosity, formation factor, tortuosity and solid density, respectively. For lithology, EST stands for Estaillade limestone, BER stands for Berea sandstone

	Sample ID	Mineral composition	k_0	ϕ	F	α_∞	ρ_s
1	EST	Mostly Calcite [33]	294	31.5	9.0	2.8	2705
2	BER12	Silica, Alumina and clays [34, 35]	48	22.9	14.0	3.2	2775
3	BER502	-	182	22.5	13.5	3.0	2723
4	DP217	Alumina and fused silica (www.tech-ceramics.co.uk)	370	45.4	4.5	2.0	3652
5	DP215	-	430	44.1	5.0	2.0	3453
6	DP82/81	-	47	41.1	5.0	2.1	3445

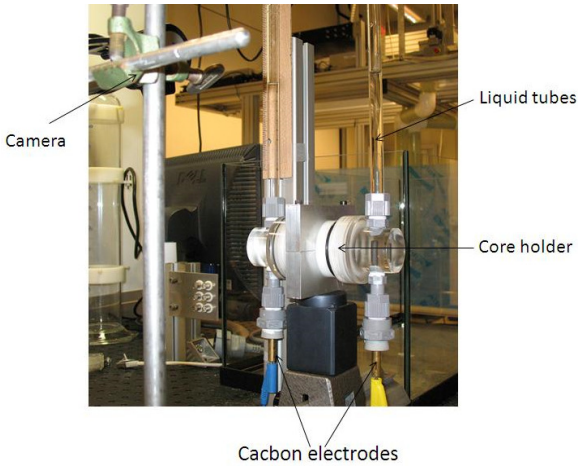

Figure 5. Experimental setup for electroosmosis measurements.

The experimental setup for the electroosmosis measurement is shown in Fig. 5. The electrodes used to apply a dc voltage across the samples are inert electrodes of graphite. Similar to the way presented by Luong and Sprik [36] to measure the maximum height difference, Δh_{max}, a camera (Philips SPC 900NC PC) with the assistance of HandiAVI software is used to take pictures of the heights of the liquid columns over time.

It should be noted that when an applied voltage exceeds a critical value (1.48V for water [37]), there will be electrolysis at the anode and the cathode. These electrode reactions produce ions and air bubbles (gas) in both electrodes. If these ions are not removed,

these reactions induce a low in pH at the anode and a high pH at the cathode and a change in electrical conductivity. Those lead to a change of the zeta potential over time and air bubbles may block the movement of fluid in capillaries. The rate of electrolysis reaction is largely determined by the current. If the current density is smaller than < 35 µA per cm^2 cross sectional area, the effects due to the electrolysis can be ignored [38]. The resistances of the fully saturated samples that we used in this paper are about 50 kΩ, so applied voltages are limited below 9 V to avoid unwanted electrolysis effects.

4. Results and discussion

Fig. 6 shows the measured maximum height difference (Δh_{max}) versus applied voltage (V) for three representative samples of EST, BER12 and DP215. We observe that there is a linear relationship between Δh_{max} and V as expected from Eq. (6) for all samples. Using the slope of the graphs in combination with Eq. (6), the expression $\frac{8\varepsilon_r\varepsilon_o|\zeta|}{\rho_f g a^2}$ is obtained as shown in Table 2.

Table 2. Calculated parameters of the samples. In which ε_r is the relative permittivity of the fluid, ε_0 is the dielectric permittivity in vacuum, ρ_f is the fluid density, g is the acceleration due to gravity, ζ is zeta potential, and a is average pore radius

	Sample ID	$\frac{8\varepsilon_r\varepsilon_o\|\zeta\|}{\rho_f g a^2}$ (mm/V)	a (µm)	ζ (mV)
1	EST	0.30	4.60	-11.2
2	BER12	0.45	2.32	-4.3
3	BER502	0.54	4.43	-18.7
4	DP217	0.75	3.65	-17.6
5	DP215	0.68	4.14	-20.5
6	DP82/81	0.95	1.37	-3.1

To determine the mean pore radius, we use the relationship between the permeability of the porous medium and the mean pore radius presented in [39] as

$$k_0 = \frac{a^2}{8F} \quad (7)$$

where k_o and F are the permeability, formation factor of the porous medium that have been shown in Table 2, respectively and a is the mean pore radius that corresponds to r_{eff} in Eq. (5) of [39]. From Eq. (7), the mean pore radius is calculated and shown in Table 2.

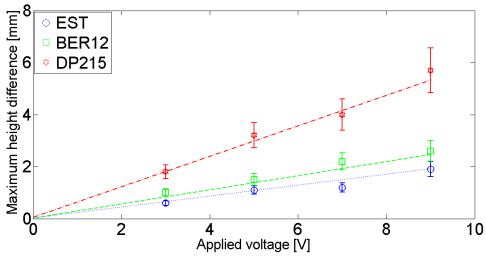

Figure 6. Maximum height difference as a function of applied voltage for three representative samples of EST, BER12 and DP215.

The expression $\frac{8\varepsilon_r\varepsilon_o|\zeta|}{\rho_f g a^2}$ and the mean pore radius a are now known. Therefore, the zeta potential is determined as shown in Table 2. In

the calculation, the product of $\varepsilon_r\varepsilon_0$ is taken as $80\times8.854\times10^{-12}$ F/s [43, 44], ρ_f is taken as 10^3 kg/m^3 and g is taken as 10 m/s^2.

There have been many papers on the zeta potential against electrolyte concentration in sandstones deduced from the streaming potential measurements. For example, Jaafar et al. [40] and Vinogradov et al. [41] reported a very high quality and comprehensive dataset of the zeta potential for sandstones as shown in Fig. 7. The zeta potential of Berea sandstone samples and artificial ceramic samples against electrolyte concentration has also been reported by Luong and Sprik [42] from streaming potential measurements as shown in Fig. 7 and Fig. 8, respectively.

Fig. 7 and Fig. 8 show that the values of the zeta potential at electrolyte concentration of 10−3 M for sandstone and ceramic samples are about -30 mV and -40 mV, respectively. Comparison between above values of the zeta potential and those shown in Table 2 shows that the values of the zeta potential deduced from our electroosmosis measurements are always much smaller than corresponding ones deduced from the reliable streaming potential measurements in literature, in particular for the low permeability samples of BER12 (6 times smaller) and DP82/81 (12 times smaller). The reasons for the difference between the values of the zeta potential obtained in our work and the ones available in literature may be that (1) the samples are not fully saturated by liquid (in particular for low permeability samples of BER12 and DP82/81), (2) the degradation of electrodes happens at voltages used in our measurements [45]. In streaming potential measurements, the samples can be easily saturated by pumping liquid through under a high pressure difference.

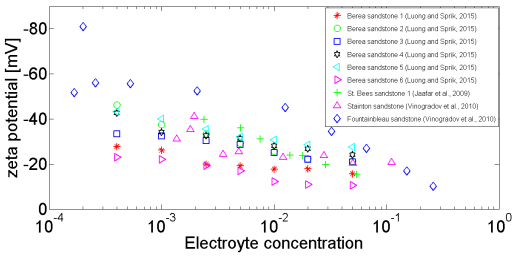

Figure 7. The zeta potential deduced from the streaming potential measurements at different electrolyte concentrations for Bees sandstone [40], Stainton sandstone and Fountainbleau sandstone [41] and Berea sandstones [42].

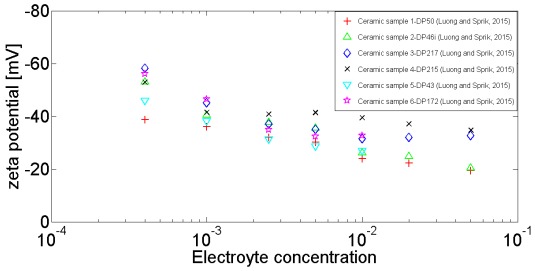

Figure 8. The zeta potential deduced from the streaming potential measurements at different electrolyte concentrations for ceramic samples [42].

It should be noted that for very high permeability samples, we need to apply high voltages to be able to observe the effect. However, when applied voltages are higher than a critical value, the electrolysis is not negligible. That leads to change of pH, electrical conductivity, and air bubbles in the pores. The result suggests that the electroosmosis measurement is not a promising method to determine the zeta potential due to the limitations mentioned above.

5. Conclusions

Electroosmosis measurements have been performed for 6 unconsolidated samples saturated with a 10^{-3}M NaCl solution to

determine the zeta potential. The comparison shows that the values of the zeta potential deduced from our electroosmosis measurements are always smaller than those of the corresponding samples deduced from the reliable streaming potential measurements in literature, in particular for the low permeability samples. The reason for the difference between the values of the zeta potential obtained in our work and the ones available in literature may be is that (1) the samples are not fully saturated by liquid (in particular for low permeability samples), (2) the degradation of electrodes happens. The result suggests that the electroosmosis measurement is not a promising method to determine the zeta potential in porous media due to the limitations mentioned above.

Acknowledgments

This work has been carried out at the Van der Waals-Zeeman Institute/Institute of Physics, University of Amsterdam. We would like to thank Boris N. Kuvshinov (Shell) for providing us the samples used in the experiments. We also would like to thank Christiaan Schoemaker for his help in improving the setups as well as measurements.

References

[1] J. Lyklema, Fundamentals of Interface and Colloid Science, Academic Press, 1995.

[2] B. Wurmstich, F. D. Morgan, Geophysics 59 (1994) 46–56.

[3] T. Ishido, J. Pritchett, Journal of Geophysical Research 104 (1999) 15247.

[4] L. Jouniaux, J. Pozzi, J. Berthier, P. Masse, Journal of Geophysical Research 104 (1999) 29293-29309.

[5] F. Fagerlund, G. Heinson, Environmental Geology 43 (2003).

[6] K. Titov, A. Revil, P. Konosavsky, S. Straface, S. Troisi, Geophysical Journal International 162 (2005) 641–650.

[7] J. H. Saunders, M. D. Jackson, C. C. Pain, Geophysics 73 (2008) 165– 180.

[8] K. Aizawa, Y. Ogawa, T. Ishido, Journal of Geophysical Research 114 (2009).

[9] R. F. Corwin, D. B. Hoovert, Geophysics 44 (1979) 226–245.

[10] F. D. Morgan, E. R. Williams, T. R. Madden, Journal of Geophysical Research 94 (1989) 12.449–12.461.

[11] A. Revil, P. A. Pezard, Geophysical Research Letters 25 (1998) 3197– 3200.

[12] G. Saracco, P. Labazuy, F. Moreau, Geophysical Research Letters 31 (2004).

[13] A. Finizola, N. Lenat, O. Macedo, D. Ramos, J. Thouret, F. Sortino, Journal of Volcanology and Geothermal Research 135 (2004) 343–360.

[14] G. Mauri, G. Williams-Jones, G. Saracco, Journal of Volcanology and Geothermal Research 191 (2010).

[15] H. Mizutani, T. Ishido, T. Yokokura, S. Ohnishi, Geophys. Res. Lett. 3 (1976).

[16] J. Pozzi, L. Jouniaux, C. R. Acad. Sci., Serie II 318 (1994) 7377.

[17] M. Trique, P. Richon, F. Perrier, J. P. Avouac, J. C. Sabroux, Nature (1999) 137–141.

[18] T. Paillat, E. Moreau, P.O.Grimaud, G. Touchard, IEEE Transactions on Dielectrics and Electrical Insulation 7 (2000) 693–704.

[19] C. Cameselle, K. R. Reddy, Electrochimica Acta 86 (2012) 10–22.

[20] C. Cameselle, S. Gouveia, D. E. Akretche, B. Belhadj, Organic Pollutants - Monitoring, Risk and Treatment, InTech, 2013.

[21] R. J. Hunter, Foundations of Colloid Science, Oxford University Press, 1986.

[22] H. M. Jacob, B. Subirm, Electrokinetic and Colloid Transport Phenomena, Wiley-Interscience, 2006.

[23] K. E. Butler, Seismoelectric effects of electrokinetic origin, PhD thesis, University of British Columbia, 1996.

[24] H. Hase, T. Ishido, S. Takakura, T. Hashimoto, K. Sato, Y. Tanaka, Geophysical Research Letters 30 (2003) 3197–3200.

[25] P. Glover, M. Jackson, The Leading Edge 29 (2010) 724–728.

[26] R. J. Hunter, Zeta Potential in Colloid Science, Academic, New York, 1981.
[27] O. Stern, Z. Elektrochem 30 (1924) 508–516.
[28] T. Ishido, H. Mizutani, Journal of Geophysical Research 86 (1981) 1763-1775.
[29] F. Reuss, Memoires de la Societe Imperiale de Naturalistes de Moscou 2 (1809) 327–336.
[30] S. Yao, J. G. Santiago, J. Colloid Interface Sci 268 (2003) 133–142.
[31] C. Rice, R. Whitehead, J. Phys. Chem. 69 (1965) 4017–4024.
[32] D.T. Luong, R. Sprik, International Journal of Geophysics Article ID 471819 (2014).
[33] E. Bemer, O. Vincke, P. Longuemare, Oil and Gas Science and Technology 59 (2004)405-426.
[34] P. Churcher, P. French, J. Shaw, L. Schramm, SPE International Symposium (1991).
[35] A. Pagoulatos, Evaluation of multistage Triaxial Testing on Berea sandstone, Degree of Master of Science, Oklahoma, 2004.
[36] D. T. Luong, R. Sprik, ISRN Geophysics Article ID 496352 (2013).
[37] D. R. Lide, CRC Handbook of Chemistry and Physics, CRC Press, 2004.
[38] D. H. Gray, J. K. Mitchell, Journal of the Soil Mechanics and foundations Division 93 (1967) 209–236.
[39] P. W. J. Glover, E. Walker, Geophysics 74 (2009) E17–E19.
[40] M. Z. Jaafar, J. Vinogradov, M. D. Jackson, Geophysical Research Letters 36 (2009) doi: 10.1029/2009GL040549.
[41] J. Vinogradov, M. Z. Jaafar, M. D. Jackson, Journal of Geophysical Research 115 (2010) doi: 10.1029/2010JB007593.
[42] D. T. Luong, R. Sprik, Submitted to Geophysical Prospecting (2015).
[43] A. Revil, P. A. Pezard, P. W. J. Glover, Journal of Geophysical Research 104(1999)20021-20031.
[44] A. Revil, H. Schwaeger, L. M. Cathles, P. D. Manhardt, Journal of Geophysical Research 104 (1999) 20033–20048.
[45] Y. Yi, Study on the degradation of carbon materials for electrocatalytic applications, Ph.D. thesis, Technical University of Berlin, 2014.

Sử dụng hiện tượng điện thẩm để đo điện thế zeta trong môi trường xốp

Lương Duy Thành[1], Rudolf Sprik[2]

[1]*Water Resources University, 175 Tây Sơn, Đống Đa, Hanoi, Vietnam*

[2]*Van der Waals-Zeeman Institute, University of Amsterdam, 1098XH Amsterdam, The Netherlands*

Tóm tắt: Điện thế zeta tại mặt phân cách giữa chất rắn và lỏng trong môi trường xốp là một tham số quan trọng trong các ứng dụng địa vật lý cũng như ứng dụng môi trường. Điện thế zeta trong môi trường xốp thường được đo bằng các kỹ thuật như điện thế chảy, dòng điện chảy. Trong bài báo này, chúng tôi sử dụng kỹ thuật điện thẩm để đo điện thế zeta cho các mẫu đá xốp gồm đá tự nhiên và đá nhân tạo được bão hòa bởi dung dịch NaCl. Kết quả đo chỉ ra rằng giá trị của điện thế zeta đo bằng kỹ thuật điện thẩm luôn nhỏ hơn nhiều so với đo bằng kỹ thuật đáng tin cậy-kỹ thuật điện thế chảy với cùng một mẫu đá xốp và dung dịch, đặc biệt đối với các mẫu đá xốp với độ thấm nước thấp. Nguyên nhân dẫn đến sự khác biệt giữa hai phương pháp có thể do các mẫu đá xốp không được bão hòa hoàn toàn bởi dung dịch NaCl hoặc do sự giảm chất lượng của các điện cực trong kỹ thuật điện thẩm. Kết quả gợi ý rằng hiện tượng điện thẩm không phải là một kỹ thuật hứa hẹn để đo điện thế zeta trong môi trường xốp.

Từ khóa: Hiện tượng điện thẩm, điện thế chảy, điện thế zeta, môi trường xốp.